Res Chem Intermed (2016) 42:3979–3998
DOI 10.1007/s11164-015-2294-9

REVIEW PAPER

Mesoporous graphitic carbon nitride materials: synthesis and modifications

Hong Li[1] · Lingzhi Wang[1] · Yongdi Liu[2] · Juying Lei[2] · Jinlong Zhang[1]

Received: 14 September 2015 / Accepted: 21 September 2015 / Published online: 12 October 2015

Abstract Graphitic carbon nitride (g-C_3N_4), as a kind of polymeric semiconductor that has unique electronic structure and excellent chemical stability, has attracted increasing attention of researchers. Moreover, the raw materials for the preparation of g-C_3N_4 are various and easily accessible. All of these have provided favorable advantages for the fast development of g-C_3N_4. Compared to bulk g-C_3N_4, mesoporous g-C_3N_4 has more prominent natures, such as high specific surface area, large pore volume, and the increased amount of surface active sites. Therefore, great efforts have been devoted to develop mesoporous g-C_3N_4 (MCN). Up to now, many methods have been explored for the synthesis of MCN, such as hard-template method, soft-template method, template-free method, sol–gel method, and so on. Among these methods, the hard template method is used most widely. In this paper, the recent research on the synthesis of MCN was reviewed. In addition, the modifications to the obtained MCN, which lead to performance enhancement of the MCN for better applications, were also summarized.

Keywords Graphitic carbon nitride · Mesoporous · Synthesis · Modification

✉ Juying Lei
leijuying@ecust.edu.cn

✉ Jinlong Zhang
jlzhang@ecust.edu.cn

[1] Key Lab for Advanced Materials and Institute of Fine Chemicals, East China University of Science and Technology, 130 Meilong Road, Shanghai 200237, People's Republic of China

[2] State Environmental Protection Key Laboratory of Environmental Risk Assessment and Control on Chemical Process, School of Resources and Environmental Engineering, East China University of Science and Technology, 130 Meilong Road, Shanghai 200237, People's Republic of China

Introduction

Recently, graphitic carbon nitride (g-C_3N_4), as a metal-free semiconductor polymer with the advantages of high chemical stability, narrow band gap (<3 eV), excellent abrasion resistance, good biological compatibility, and so forth, has become a new star in the field of materials [1]. g-C_3N_4 is one kind of C_3N_4, which have five kinds of structures: the alpha phase, the beta phase, the cubic phase, the quasi cubic phase, and the graphite phase. Similar to graphite, g-C_3N_4 also has a sheet structure, which contains C_3N_3 rings and C_6N_7 rings. The rings connect with each other by the N in the end to form an unlimited plane. With the highly conjugated electron pair of N and the unique band gap structure [2], g-C_3N_4 has shown potential application prospects in many fields, such as hydrogen production from water splitting [3], reduction of carbon dioxide [4], degradation of organic pollutants [5, 6], oxidation of alcohols [7], optical sensors, and others. Many materials have been reported that can be used to synthesize g-C_3N_4, e.g., cyanamide, dicyandiamide, melamine, urea, ammonium thiocyanate, and hexamethylenetetramine. The methods to prepare bulk g-C_3N_4 are also various, including high-temperature calcination [8, 9], shock wave compression [10, 11], high-pressure pyrolysis [12], ion implantation [13], low-energy ion radiation [14], ion beam deposition [15, 16], sputtering [17], chemical vapor deposition [18, 19], laser pulse [20, 21], etc. With deeper study, the methods for preparation and characterization of bulk g-C_3N_4 have been quite mature. However, general defects of bulk materials like small specific surface area and less active sites block the further development of bulk g-C_3N_4.

Mesoporous material is a hot topic in recent decades. Mesoporous materials are famous for the 2–50-nm pore channels inside them, which make them have more excellent properties and potential applications than bulk materials [22–24]. Generally speaking, mesoporous materials have many excellent properties of super high specific surface area, ordered pore structure, lower density, more active sites, and strong adsorption ability [25–27]. Therefore, mesoporous material has attracted widespread interest in multidisciplinary studies since the study has begun. Making carbon nitride into mesoporous material is good for its catalytic activity, increasing the active sites, improving the utilization rate of photons, and promoting further research and extensive usage of g-C_3N_4 materials. Therefore, great efforts have been made to prepare and study mesoporous g-C_3N_4 (MCN). In this review, we will do a simple review on the development of MCN in recent years from the aspects of preparations and modifications. Firstly, we would like to introduce four main kinds of methods for the preparation of MCN, including hard-template method [28], soft-template method [29], template-free method [30], and sol–gel method [31]. These methods use different strategies and precursors, obtaining products with different pore regularity and other properties. Then, the modifications to MCN, which can lead to catalytic performance improvement and application scope broaden, will be presented. Finally, we will give a short summary on the development of MCN and outlook for the application prospects of MCN.

The preparation of MCN

Bulk g-C_3N_4 can be synthesized easily from the direct thermal polymerization of precursors at high temperature in air. The kinds of the precursors are very rich, including cyanamide, dicyandiamide, melamine, urea, ethidene diamine, carbon tetrachloride, ammonium thiocyanate, hexamethylenetetramine, etc. The main reactions occur for the precursor in the process of high-temperature polymerization is as shown in Fig. 1 [30], which is represented by that of cyanamide.

The reactions are a combination of polyaddition and polycondensation. At first, the precursors polymerize to melamine. Secondly, condensation occurs by eliminating ammonia from melamine to form the g-C_3N_4 polymer. This sequence is schematically shown in Fig. 1 [30]. X-ray analysis and differential scanning calorimetry (DSC) studies demonstrated that in the process of the thermal polymerization, essentially melamine-based products can be found at 350 °C, while the melamine rearrange to form tris-*s*-triazine at around 390 °C. Condensation of the tris-*s*-triazine unit to polymers, networks, and potentially the final g-C_3N_4 occurs at around 520 °C, with the material becoming unstable slightly above 600 °C. Heating to 700 °C results in the residue-free disappearance of the material via generation of nitrogen and cyano fragments. This reaction process may have a relationship with the cohesive energy. Theoretical calculations reveal that the

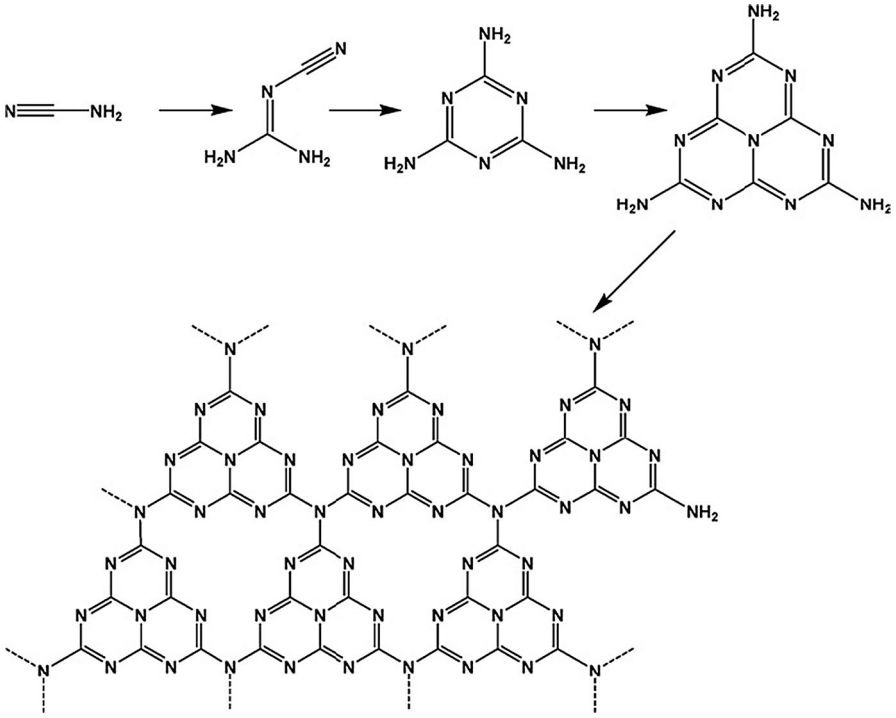

Fig. 1 Reaction path for the formation of g-C_3N_4 using cyanamide as the precursor [30]

cohesive energy of the molecules increases along with the polyaddition path as shown in Fig. 2 [30].

The preparation of MCN includes the above-mentioned reactions for the preparation of bulk g-C_3N_4 and an additional step to generate mesopores. The methods to prepare MCN are not very abundant, which have been reported as the following several kinds.

Hard-template method

In this method, the templates with mesopores are pre-synthesized, which are usually mesoporous silica materials. The precursor solution of g-C_3N_4 is perfused into the mesopores of the template and the precursor will transfer into g-C_3N_4 in the pore channels by heating to a high temperature. After a carving treatment of the template, MCN can be obtained.

Vinu et al. synthesized MCN by a typical hard template method. In their synthesis, mesoporous silica SBA-15 [32] was added to a mixture of ethylenediamine and carbon tetrachloride. After the reflux of the mixture followed by a calcination, MCN with uniform pores and high photocatalytic activity was obtained [33]. Zhao et al. also synthesized MCN by using SBA-15 as a hard template. In their results, the specific surface area and pore volume as well as N content of the obtained MCN were tightly related with the chosen precursor. By using hexamethylenetetramine as the precursor, highly ordered MCN with ultrahigh specific surface area (1116 $m^2\ g^{-1}$) and pore volume (1.54 $cm^3\ g^{-1}$) was obtained. The procedure for the preparation is illustrated in Fig. 3 [34]. Besides changing the precursor, it was demonstrated by Vinu et al. that the specific pore volume and the pore diameter can also be controlled by the simple adjustment of the structure of the SBA-15 template. They successfully prepared MCN with tunable pore diameters by using SBA-15 materials with different pore diameters as templates through a simple polymerization reaction between ethylenediamine and carbon tetrachloride. The results showed that the pore diameter of the MCN materials can be easily tuned from 4.2 to 6.4 nm without affecting their structural order. Moreover, they also controlled the nitrogen content of the MCN materials by the simple adjustment of the ethylenediamine-to-carbon tetrachloride weight ratio [35].

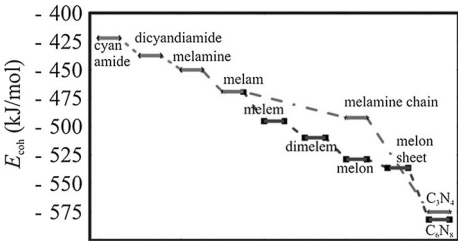

Fig. 2 Calculated energy diagram for the synthesis of g-C_3N_4. Cyanamide as the starting precursor is firstly condensed into melamine. Further condensation can then proceed via the triazine route (*dash-dot line*) to C_3N_4, or melamine can form melem and then follow the tri-*s*-triazine route (*dashed line*) to form C_6N_8 [30]

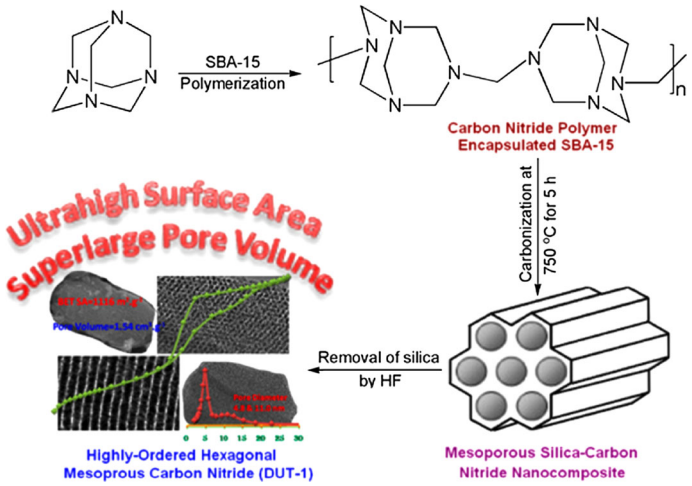

Fig. 3 Schematic illustration of synthetic procedure for highly ordered MCN material by using SBA-15 as a hard template and hexamethylenetetramine as the precursor [34]

In addition to SBA-15, other kinds of mesoporous silica materials have also been applied as templates for the synthesis of MCN. Vinu et al. prepared MCN with cage-type mesopores through a straightforward polymerization of ethylenediamine and carbon tetrachloride inside the pore channels of mesoporous silica FDU-12. The obtained MCN materials were used as adsorbents for the capture of CO_2 molecules at different high pressures and temperatures. The materials showed excellent affinity towards CO_2 molecules because of the strong acid base interactions [36]. Sang-Eon Park synthesized MCN with hexagonal platelet morphology by using disk-type mesoporous silica (INC-2) as a hard template and melamine as a precursor. This material possessed high nitrogen content in the framework and surface, which provides potentially Lewis base sites for Knoevenagel condensation [37]. Mori et al. demonstrated the preparation of MCN with 3D porous structure and high nitrogen content by employing a mesoporous silica KIT-6 as the template and a cyclic aromatic compound 3-amino-1,2,4-triazine as the precursor. One of the important features of this work is that the cyclic aromatic precursor helped to preserve the nitrogen in the carbon matrix of the final product even after the carbonization process [38]. Vinu et al. also prepared 3D MCN using mesoporous silica KIT-6 as hard template, and ethylenediamine and carbon tetrachloride as the sources for N and C, respectively. The obtained materials possessed bimodal pores that can be controlled with a simple adjustment of the pore diameter of the KIT-6 templates [39]. The synthesis steps are shown in detail in Fig. 4.

Since most studies used amorphous mesoporous silica materials as hard templates, Chari et al. reported for the first time the utilization of mesoporous silica nanoparticles as the template. The obtained product was well-ordered MCN nanoparticles with a size smaller than 150 nm and high nitrogen content (C_4N_2) that is twice that of the MCN prepared from mesoporous silica SBA-15 [7].

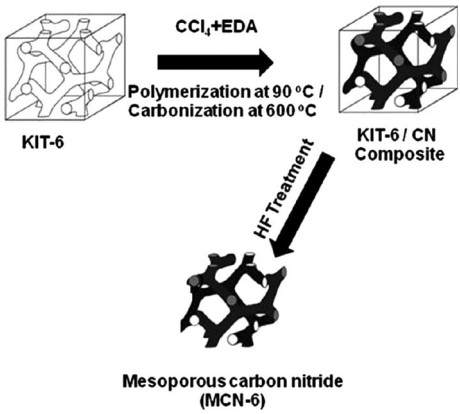

Fig. 4 Schematic representation for the synthesis of MCN using mesoporous silica KIT-6 with 3D porous structure as hard templates [39]

The hard-template method for preparing MCN can keep the original structure properties of the template materials, so we can design the morphology and the pore structure of the target MCN through designing the hard template. The MCN materials prepared by this method generally have highly ordered 2D or 3D nanopores and good thermal stability. Therefore, the hard template method is currently the most used. There are, however, some inherent drawbacks of this method that are difficult to overcome. For instance, the precursors of the product must be liquid or soluble in some polar solvent for the perfusion. Otherwise, the perfusion will be difficult. The products will form on the surface of the template rather than in the pore channels. Moreover, the removal of the hard template usually needs the use of hydrofluoric acid, or NH_4HF_2, or a strong base that is highly corrosive and has the requirement for high experimental safety.

Soft-template method

Soft-template method generally refers to the method that uses surfactant, amphiphilic polymer, or other organic molecules as the template. The mesophase usually forms by the self-assembly of the template and the precursor in the reaction solution.

Fan et al. synthesized MCN with bimodal pore distribution by using a surfactant Triton X-100 as the soft template and melamine and glutaraldehyde as precursors through polymerization and carbonization. The sizes of the mesopores in the product were centered at 3.8 and 10–40 nm [29]. Yan et al. reported a novel method to synthesize MCN, in which the block polymer Pluronic P123 was used as soft template and melamine was used as the precursor. The melamine and Pluronic P123 were dispersed into distilled water together. After a series of processes including refluxing, adding sulfuric acid solution, drying and calcination, the mesoporous product was obtained. The product was MCN with worm-like mesopores as observed by the HRTEM image presented in Fig. 5. The pore size distributions calculated by the Barret–Joyner–Halender (BJH) method displayed different characteristics for the products prepared without and with P123, as shown in

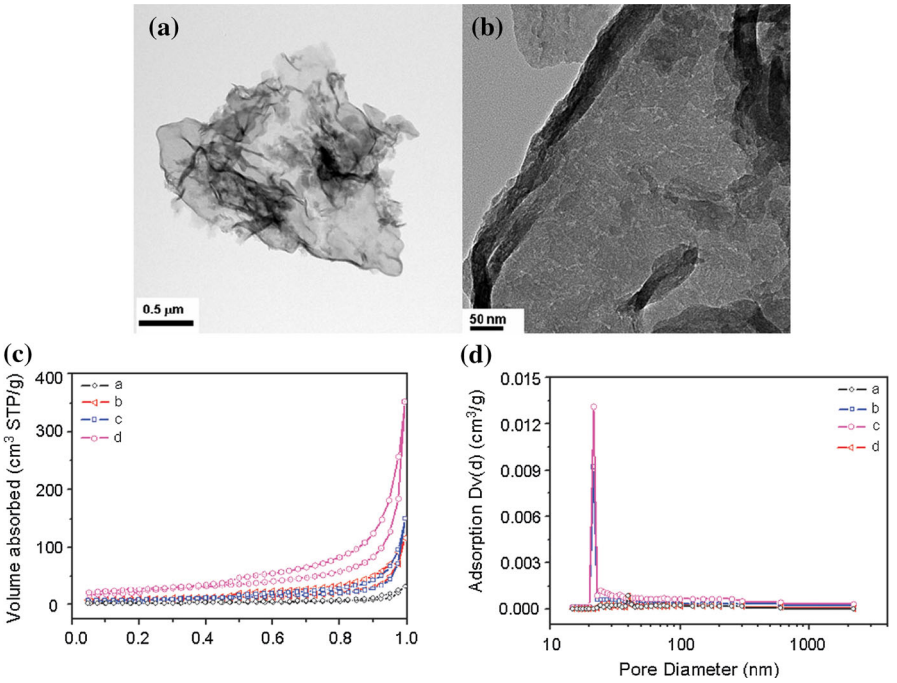

Fig. 5 *Low* magnification (**a**) and *high* magnification (**b**) TEM images of the MCN prepared by using Pluronic P123 as soft template. (**c**) N_2 adsorption/desorption isotherm and (**d**) corresponding pore-size distribution of MCN prepared without (*lines a*, *b*) and with (*lines c*, *d*) P123 [40]

Fig. 5. The pore-size distributions are very broad for the former, while they are highly uniform and narrow for the latter [40].

Li et al. developed a facile soft template method for the synthesis of boron- and fluorine-doped MCN. They found that the commercially available room-temperature ionic liquid, 1-butyl-3-methylimidazoliumtetrafluoroborate ($BmimBF_4$) is a unique soft template for the synthesis of boron- and fluorine-enriched MCN, in which an organic precursor, for example dicyandiamide (DCDA), self-condensed to form carbon nitride solids in the presence of $BmimBF_4$. Their results demonstrated that ionic liquids are good soft templates, which are generally defined as organic salts with a low melting point, usually below 100 °C. They inherit many features of inorganic molten salts, such as excellent chemical and thermal stability and negligibly small vapor pressure, with the convenience of being liquid under ambient conditions [41].

The soft template method has less synthetic procedures than the hard template method. It has advantages such as simple equipment, easy operation, and low cost. The exploration of new template is important for the further application of the soft template method for the preparation of MCN. Meanwhile, the soft template method has the disadvantage that it cannot always strictly control the size and morphology of the mesoporous products, resulting in limitations of the catalytic performance of the final MCN products.

Template-free method

This method does not need other substances to be used as templates. By simply controlling the experimental conditions or selecting appropriate precursors, mesopores can be produced in the products.

Lu et al. reported an easy method to prepare MCN by directly pyrolyzing urea without templates at ambient conditions. In their experiment, urea powder was put into an alumina crucible with a cover and heated to 600 °C in 1 h, then maintained in this temperature for 4 h. The resultant powder was washed with water and anhydrous ethanol thoroughly, and then collected by filtration and dried at room temperature. The MCN possessed a layered structure and abundant mesopores, as shown in Fig. 6a. The pore size is in the range of 20–40 nm (Fig. 6b) [42].

Different from generating pores in the synthesis process of g-C_3N_4 as mentioned above, Shanker et al. developed a template-free strategy to synthesize MCN by a post-ultrasonic treatment of bulk g-C_3N_4. In their method, the bulk g-C_3N_4 is dispersed in a mixed solvent of ethanol–water (1:2) and then sonicated at ambient temperature for 5 h. Porous g-C_3N_4 sheet possessing high surface area and large pore volume was obtained. More attractively, the photocatalytic activity of the MCN was much higher compared to bulk g-C_3N_4 under visible-light irradiation. In addition, the high reusability of the synthesized MCN could meet the requirement of suitable candidates for practical photocatalytic applications [43].

The template-free method is the most ideal method for the preparation of MCN. First of all, it is a simple method, because the operation procedure is without a lengthy preparation process, saving time and saving raw materials. Secondly, it is a kind of environmentally friendly method. Because no template is used, no toxic template etchant needs to be used. Therefore, it is a kind of green synthesis method. However, similar to the soft template method, the pore structure in the products cannot achieve a high degree of order and it is difficult to design and control the properties of the pores. In addition, there are more stringent requirements in the heating process and the selection of raw materials.

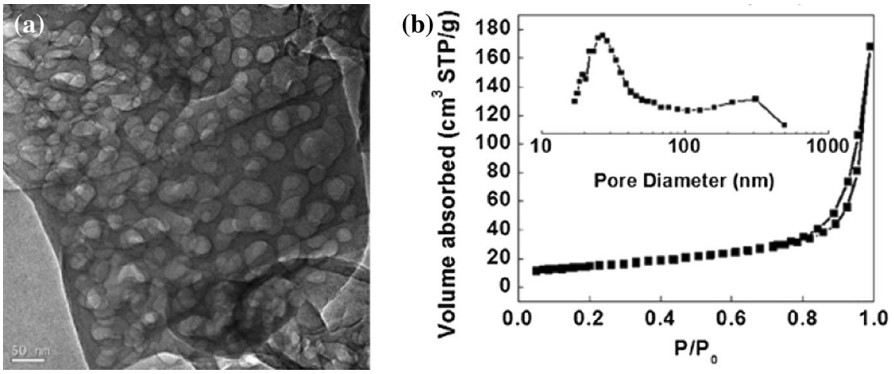

Fig. 6 (**a**) TEM image of MCN prepared by pyrolyzing urea without templates. (**b**) N_2 adsorption/desorption isotherm and pore-size distribution (*inset*) of the obtained MCN [42]

Sol–gel method

The sol–gel method is a commonly used method for the preparation of nanomaterials. In the sol–gel method for the preparation of MCN, the precursors of g-C_3N_4 will be mixed with the precursor of silica or a sol of silica. After a series of processes including consecutive sol mixing, gel formation, calcinated polymerization, and silica removal, the target MCN can be obtained. Similar to the hard template method, this method needs a step for the removal of the template. However, different from the hard template method, the silica template is formed during the preparation process of g-C_3N_4 rather than pre-synthesized.

Sun et al. synthesized MCN through adding the silica precursor tetraethyl orthosilicate (TEOS) into the cyanamide hydrochloride solution followed by in situ formation of g-C_3N_4/SiO_2 composite by thermal polymerization. After removing the silica in the composite, MCN was obtained. The process of the synthesis and the TEM image of the product are shown in Fig. 7. It was obviously seen that a great number of mesopores (labeled by red circles) were formed in the MCN sample. The pore diameter was approximately 5 nm. The obtained MCN possessed a large surface area and enhanced photocatalytic degradation performance for Rhodamine B pollutant under visible light irradiation [44].

Thomas et al. also prepared MCN by a sol–gel approach. Cyanamide and TEOS were used as the precursor for g-C_3N_4 and silica, respectively, and were mixed in an acidic ethanol solution. After condensation and heat treatment, it was observed that the carbon nitride and silica formed highly interpenetrating mesophases, which led to the formation of MCN or mesoporous silica after selective removal of either of the phases. The process is shown in detail in Fig. 8. Importantly, the carbon nitride preserved its graphitic stacking even in the spatial confinement introduced by the surrounding silica phase. As TEOS is liquid and cyanamide can be dissolved to be liquids, this approach allowed convenient shaping into thin and thick films or monoliths of mesoporous carbon nitrides [45].

Besides the alkoxy silane precursor, silica sol was directly used as a starting material in the sol–gel method. Antonietti et al. synthesized MCN using Ludox-HS 40 silica dispersion and cyanamide as a precursor. The cyanamide was completely

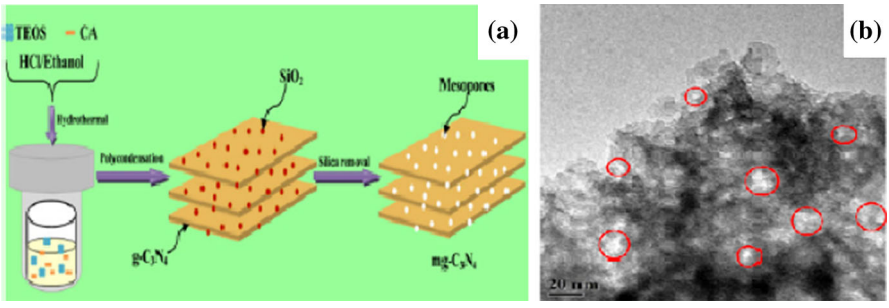

Fig. 7 (**a**) Schematic illustration of the preparation of MCN by a sol–gel method using TEOS and cyanamide hydrochloride. (**b**) TEM image of the obtained MCN [44]

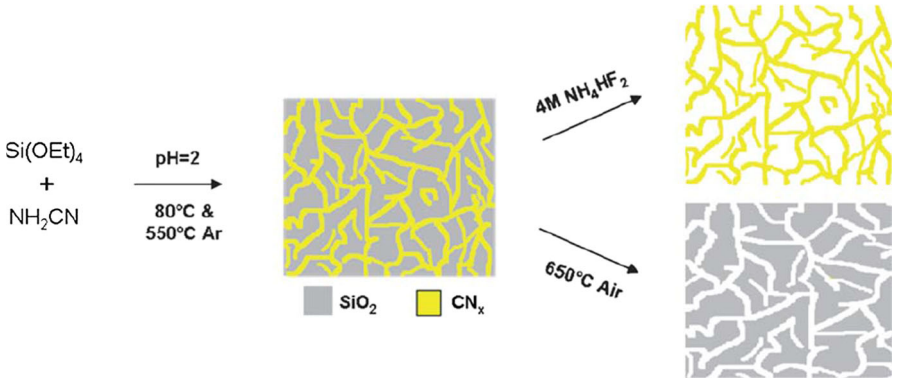

Fig. 8 The sol–gel route to obtain mesoporous carbon nitride and silica using cyanamide and TEOS as precursors [45]

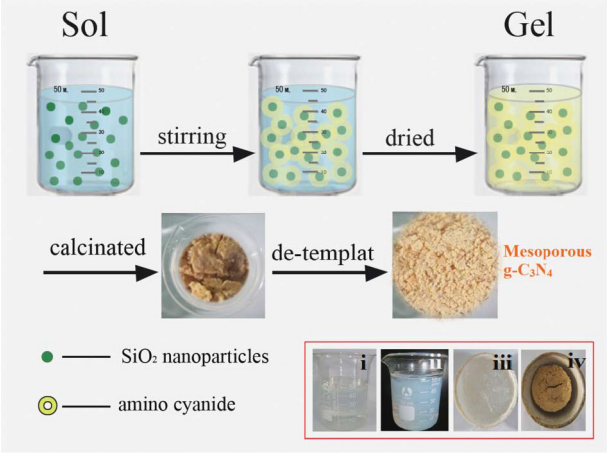

Fig. 9 Schematic mechanism for the formation of MCN by sol–gel process using Ludox-HS 40 silica dispersion and cyanamide [46]

dissolved into Ludox-HS 40 silica dispersion, forming a homogeneous and viscous solution, which was then dried at 70 °C for 1 h to get a transparent gel. The gel was transferred into a porcelain boat and calcinated at 550 °C for 4 h under N_2 atmosphere. After that, the sample was treated with a 4 M NH_4HF_2 solution to remove the silica template. Finally, yellow powders of MCN were harvested. The mechanism for the formation of the MCN is shown in Fig. 9 [46]. Similar methods using Ludox-HS 40 silica to prepare MCN were also reported by Wang et al. [47] and Shiraishi et al. [48].

MCN with bimodal pore systems were also prepared by the sol–gel method [49]. In this work, guanidinium chloride and 12 nm colloidal silica were used as the starting materials. A series of MCN samples with bimodal pore systems (1.8 and

13.4 nm), and high surface areas along with large pore volumes have been successfully prepared by using different silica/GndCl ratio. The results of the work revealed that with the increase of silica/GndCl ratios from 0.4 to 1.0, the surface areas and pore volumes increased progressively. In addition, using a higher amount of silica template would be favorable to the volatilization in calcinations of GndCl. As a result, lower nitrogen content was achieved as the weight ratio of silica/GndCl was increased continuously. Therefore, it was demonstrated that in this sol–gel method, by simply adjusting the adding ratio of silica/GndCl, the surface area, pore volume, and C/N ratio of the MCN product can be tuned.

The sol–gel method is a simple, efficient, and viable technique for the large-scale production of MCN. This proposed technique also allows controlled development and tailored design of the pore structures, which is of crucial importance for the application of MCN. Meanwhile, some problems have be overcome for this method. For example, it usually takes a very long time in the whole sol–gel process. What's more, the removal of the silica template makes the overall synthesis procedure relatively tedious and environmentally unfriendly.

Carbon nitride is a new kind of environmentally friendly catalyst, and it is in the golden period of rapid development. Many scholars are doing comprehensive study from all aspects. With the passage of time and the development of new technologies, the more excellent method for the preparation of MCN is believed to appear.

The modifications of MCN

The unique electronic structure along with the advantages from the mesoporous texture makes MCN efficient heterogeneous catalysts for many reaction systems. Besides, in situ or post-modifications to the MCN can lead to further catalytic performance enhancement or application scope broadening of the material. For instance, when MCN is applied as a photocatalyst, proper modifications can greatly enhance its photocatalytic activity. On one hand, the modifications can reduce the recombination of electron and hole pairs, which can improve the quantum efficiency of the photocatalysis; on the other hand, the modifications can make the absorption wavelength take a red shift and thus broaden the absorption spectrometry, resulting in better utilization of sunlight. At present, there are various modification methods for MCN. The representative and typical modification methods can be divided into five categories: nonmetal doping, noble metal loading, metallic oxide loading, dye photosensitization, and polyoxometalates immobilization.

Non-metal doping

In this kind of modification, the non-metal elements are usually doped into the C–N matrix of the MCN material. After modification, the material stays metal-free and its catalytic performance is enhanced.

Li et al. developed boron- and fluorine-enriched MCN by using room-temperature ionic liquid, 1-butyl-3-methylimidazoliumtetrafluoroborate ($BmimBF_4$)

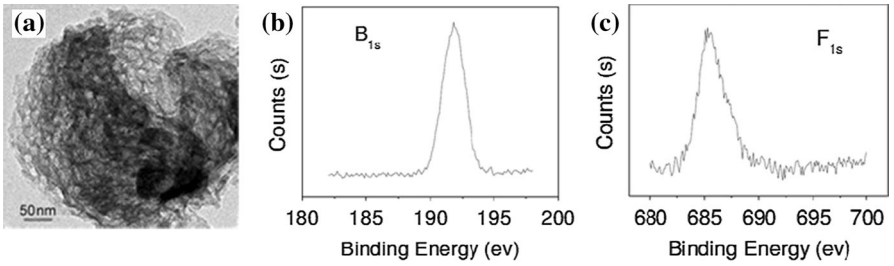

Fig. 10 (**a**) Typical TEM image of boron- and fluorine-doped MCN. (**b**), (**c**) XPS patterns of B_{1s} and F_{1s} in the doped MCN [50]

as a soft template for the mesopores as well as a source for the boron and fluorine dopant [50]. The resulting materials possessed a well-developed, sponge-like mesopore structure, as shown in Fig. 10a, and X-ray photoelectron spectroscopy (XPS) analysis (Fig. 10b, c) demonstrated that both boron and fluorine atoms have been incorporated into the CN matrix. The boron content was about 20 mol%, while the fluorine content was about 4 mol%. It was proposed that the B atoms entered C sites in polymeric C–N structures (thus balancing stoichiometry), with F saturating residual bonds. The material exhibited excellent photoconductivity under visible light and efficiently catalyzed the oxidation of cyclohexane. Furthermore, this doped MCN is expected to give excellent results in other organic reactions, as it has a large surface area and suitable pore volume with a large number of boron functional groups on the surface, which might act as strong Lewis acid sites, thus complementing the basic nitrogen sites. In addition, their ionic-liquid-based strategy could be extended to incorporate other heteroatoms in MCN material by changing the anion or cation of the ionic liquids.

Although a large number of studies have dealt with the non-metal doping of bulk g-C_3N_4 materials [51, 52], the research on the non-metal doping of MCN is still in its infancy, probably due to the difficulty of simultaneously realizing the generation of mesopores and the doping of non-metal elements into the C–N matrix.

Noble metal loading

Because the noble metals have different Fermi levels from MCN, noble metal loading can change the distribution and transmission of electrons in the catalyst. After the contact between the noble metal and MCN, the electrons can transfer from the higher Fermi level to the lower one. When the two materials get together, electrons can transfer from MCN to the noble metal, and the holes can transfer from noble metal to MCN until both Fermi levels reaching balance. So the photo-generated electrons and holes gather on noble metal and MCN surfaces, respectively. Then the electrons and holes can be used to promote different redox reactions.

Vinu et al. [53] grew Au nanoparticles into MCN by reduction of $HAuCl_4$ at the condition of $NaBH_4$ for the first time (Fig. 11a). Au nanoparticles with a size of

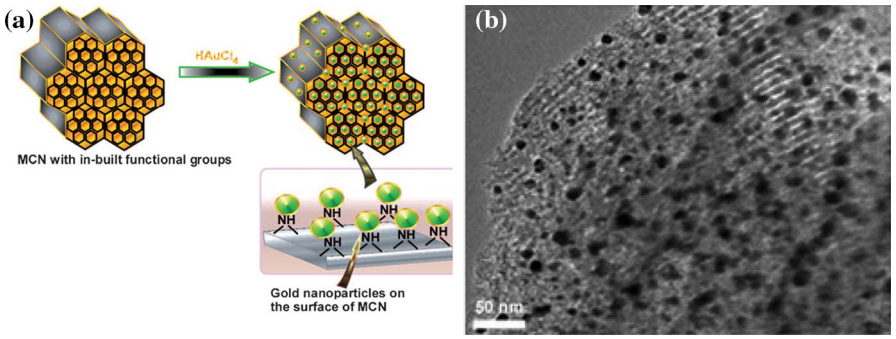

Fig. 11 (**a**) Schematic illustration for the growth of Au nanoparticles into MCM and (**b**) HRTEM images of the Au@MCN composite [53]

<7 nm were highly dispersed on the inner surface of MCN. No agglomeration of the Au nanoparticles was observed from the HRTEM image of the composite (Fig. 11b). The MCN was demonstrated to act as a stabilizing, size-controlling, and reducing agent for the Au nanoparticles. The experiment results demonstrated that the Au@MCN composite was a highly active, selective, and recyclable catalyst for the three-component coupling reaction of benzaldehyde, piperidine, and phenyl acetylene for synthesis of propargylamine.

Wang et al. [54] loaded Pd nanoparticles on MCN to prepare a novel catalyst, which was proved to be highly active and selective for the direct hydrogenation of phenol to cyclohexanone. From the STEM, HRTEM, and TEM images presented in Fig. 12, it can be observed that the Pd nanoparticles were highly dispersed on the MCN. The average size of the Pd nanoparticles is ~5 nm, as demonstrated by the size distribution in Fig. 12d. The catalyst exhibited a high activity for the hydrogenation of phenol to cyclohexanone. The high catalytic activity was attributed to the special structure of the semiconductor–metal heterojunction between Pd and MCN, which led not only to a uniform dispersion of Pd but also to additional electronic activation of the metal nanoparticles and a "nonplanar" adsorption of phenol. Therefore, the fast and selective hydrogenation of phenol to cyclohexanone was realized.

In addition to Au and Pd nanoparticles, Pt nanoparticles were also homogenously loaded in the ordered mesoporous channels of MCN, which was reported by Wen-sheng Dong et al. [55]. The synthesized materials were applied in the selective oxidation of glycerol with molecular oxygen in base-free aqueous solution. The catalysts showed high conversion efficiency and selectivities. Sun et al. [56] also prepared similar composites of MCN and Pt nanoparticles. Pt nanoparticles with a diameter of 3–4 nm were synthesized on the MCN support, and the composites were applied as bifunctional air electrodes. The electrochemical performances of the electrodes were examined with an all-solid-state Li-air battery, and improved results with good round-trip efficiency as high as 87 % were obtained.

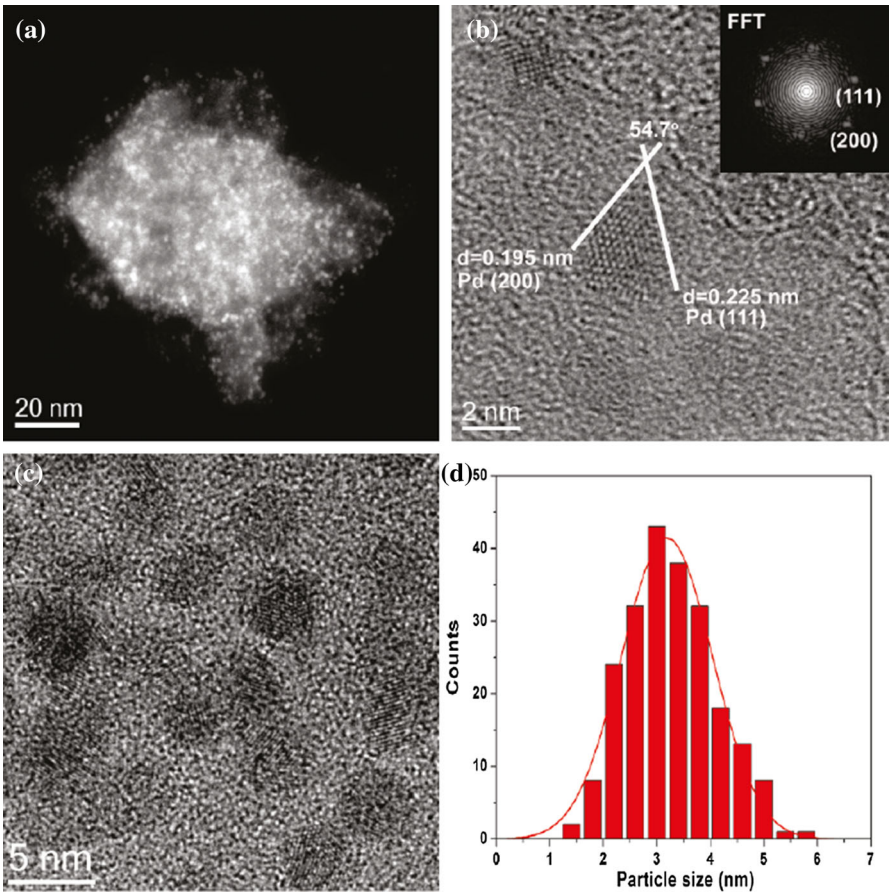

Fig. 12 (**a**) STEM, (**b**) HRTEM, and (**c**) TEM images, and (**d**) particle size distribution of Pd@MCN. The *inset* in (**b**) is the local fast Fourier transform [54]

Metallic oxide loading

In addition to the noble metal loading, the metallic oxide has also been loaded into the mesoporous channels of MCN. The metallic oxide loading can improve the photocatalytic activity of MCN by forming a heterojunction catalyst, which can increase the separation rate of photogenerated charges.

Kailasam et al. developed mesoporous carbon nitride–tungsten oxide composites (MCN/WO_3), and applied it into photocatalytic hydrogen evolution. MCN/WO_3 showed very high photocatalytic activity for the evolution of hydrogen from water under visible light and in the presence of sacrificial electron donors. The higher activity could be attributed to the high surface area and synergetic effect between the carbon nitrides and the WO_3, which resulted in improved charge separation through a photocatalytic solid-state Z-scheme mechanism [57]. The detailed mechanism is shown in Fig. 13. After modification with WO_3, the photo-generated

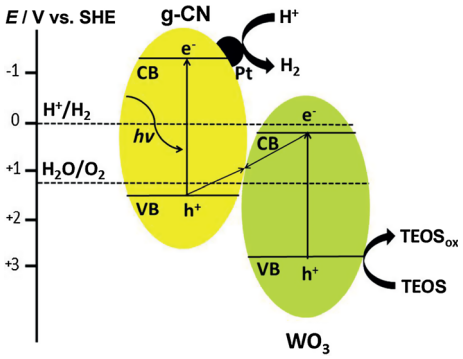

Fig. 13 Schematic illustration of the solid-state Z-scheme photocatalytic mechanism in MCN/WO_3 composites [57]

holes in the valance band of g-C_3N_4 and the photo-generated electrons in the conduction band of WO_3 would recombine at the interface, leaving the electrons in the conduction band of g-C_3N_4 and holes in the valance band of WO_3. Therefore, the overall charge separation efficiency was improved, leading to better photocatalytic activity [57].

Xu et al. prepared vanadia-modified MCN catalysts using NH_4VO_3 as a precursor and mesoporous carbon nitride as a support through a wet impregnation method. The modified MCN materials showed remarkable catalytic performance in the hydroxylation of benzene to phenol in the presence of H_2O_2. The high catalytic activity is attributed to high benzene-activation capability of MCN and dispersion of vanadia species. Owing to the inbuilt and unique tri-*s*-triazine moieties, MCN chemically adsorbed and then activated benzene on the catalytic surface, via an electron transfer from HOMO of C_3N_4 to LUMO of benzene, wherein MCN materials featuring high surface areas and rich pores upgraded the amount of adsorbed benzene molecules. On the other hand, H_2O_2 oxidized V^{4+} species that dispersed on the surface of MCN to radical-containing V^{5+} species, simultaneously generating H_2O. The as-produced V^{5+} species reacted with the activated benzene and thus yielded the target phenol. The possible pathway is shown in Fig. 14 [58].

Dye photosensitization

Dye photosensitization refers to the dye molecules adsorbing on the surface of the photocatalyst by chemical or physical interactions, making the light absorption of the catalyst to a longer wavelength range, thereby expanding the excitation wavelength response range [59]. Dye sensitization generally involves three basic processes: (1) the dye molecules are adsorbed onto the surface of the photocatalyst; (2) the adsorbed dye molecules absorb a photon to be excited; (3) the excited dye molecules inject electrons into the conduction band of the photocatalyst. If the oxidation level of dye molecules is more negative than the conduction band energy level of the semiconductor, dye molecules in excited states can transfer electrons to the conduction band of the semiconductor. Then the semiconductor can accept an

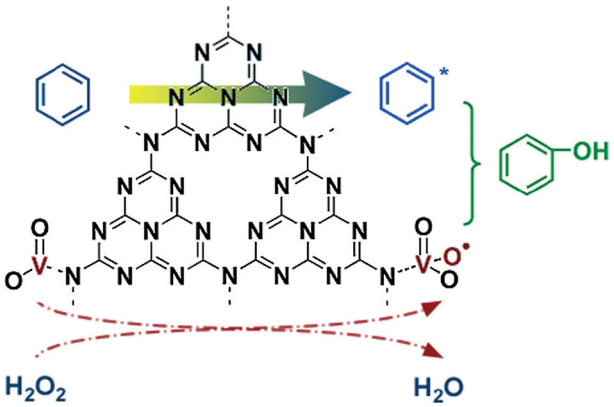

Fig. 14 A possible reaction mechanism for the hydroxylation of benzene catalyzed by vanadia-modified MCN [58]

electron from the excited dye molecule and transfer it to the O_2 adsorbed on the surface to generate active species. Through the above process, the semiconductor obtains better catalytic activity.

Min et al. demonstrated that the photo response of the MCN can be greatly extended up to nearly 600 nm by sensitization with Eosin Y (EY), as shown in Fig. 15a. This sensitized MCN was demonstrated to have high photocatalytic activity for H_2 evolution under visible light irradiation, especially in the longer wavelength regions (450–600 nm) (Fig. 15b). In addition, the light-absorption property of the photosensitizer governs the reaction rate. These results indicated that efficient electron transfer between excited EY molecules and MCN was achieved. The mechanism for photocatalytic H_2 evolution on the EY-MCN catalyst is shown in Fig. 15c. Moreover, the MCN with high surface area and mesoporous structure can greatly facilitate the adsorption of EY molecules on the surface, thus promoting the activity via improved light harvesting [42].

Antonietti et al. investigated spectral sensitization of MCN photocatalyst by depositing magnesium phthalocyanine (MgPc) to expand the absorption wavelengths to that longer than those of the original MCN. The obtained sample, MgPc/Pt/MCN (Pt as a cocatalyst), showed stable photocatalytic evolution of H_2 from aqueous solution in the presence of sacrificial reagents (triethanolamine), even under irradiation at wavelengths longer than 600 nm [60]. The diagram depicted in Fig. 16 showed that the photo-excited electrons on MgPc were most likely transferred through the conduction band of MCN to Pt. It is therefore reasonable to consider that the MgPc molecules that were not in contact with MCN would be incapable of efficient charge transfer from MgPc to MCN, and dye (MgPc) to dye (MgPc) charge transfer would not occur smoothly. Therefore, a monolayer of dye molecules on the photocatalyst maximizes the overall photocatalytic efficiency.

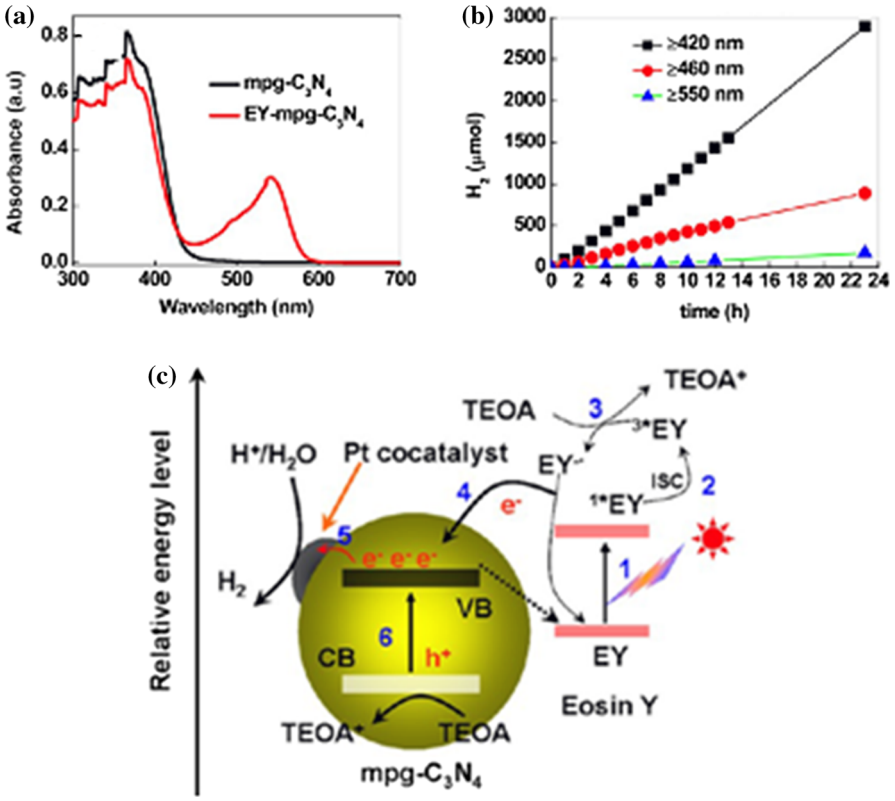

Fig. 15 (**a**) UV–Vis diffuse reflectance spectra of MCN and EY-MCN. (**b**) Time courses of photocatalytic H_2 evolution over EY-MCN/Pt photocatalyst under different wavelengths of light irradiation. (**c**) Photocatalytic mechanism for H_2 evolution on EY-MCN/Pt photocatalyst under visible light [42]

Polyoxometalates immobilization

Polyoxometalates are well-known inorganic compounds, which have attracted wide attention due to their special functions [61, 62]. One of the most notable features of polyoxometalates is that they simultaneously have acidic and oxidizing capabilities. In addition, by changing the elements of the polyoxometalate cluster, the catalytic properties can be managed and changed. Therefore, as acidic or oxidized or dual-function catalysts, polyoxometalates are widely used in various reaction systems. The polyoxometalate immobilized to the surface of MCN can form a synergistic effect from the combination of catalytic advantages of polyoxometalates and MCN, which can greatly improve the catalytic performance.

Xie et al. [62] immobilized polyoxometalate complex $[Co_4(H_2O)_2(PW_9O_{34})2]_{10}$ (CoPOM) in ordered MCN by an vacuum-assisted impregnation as shown in Fig. 17a. The high surface area of MCN support offered a perfect and stable dispersion of CoPOM. The obtained composite was demonstrated to work as a highly

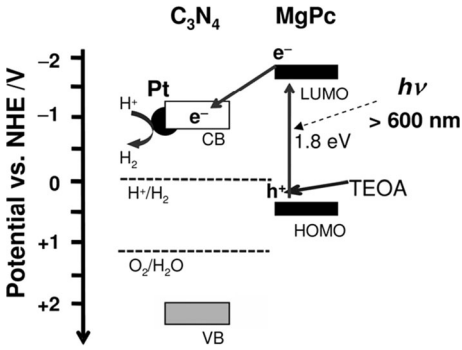

Fig. 16 Electron-hole transport in MgPc/Pt/MCN photocatalysts [60]

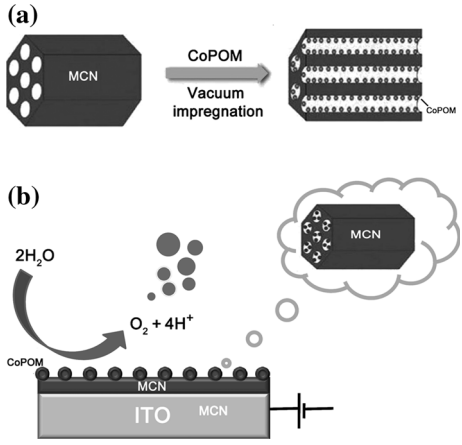

Fig. 17 (**a**) Preparation of a CoPOM/MCN composite by vacuum-assisted impregnation. (**b**) Scheme for using CoPOM/MCN composite as water oxidation catalyst [62]

efficient water oxidation catalyst. This may be because anchoring CoPOM to the support material MCN can improve electrical contact between the redox-active centers and the surface of the electrode. In addition, it is likely that the carbon nitride environment plays an important role for sustaining activity by protecting the active cobalt centers of the catalyst from deactivation by surface restructuring.

Zhu et al. prepared phosphotungstic acid/MCN catalyst by immobilizing phosphotungstic acid ($H_3PW_{12}O_{40}$, HPW) on MCN. The HPW/MCN catalyst showed high catalytic activity in the oxidative desulfurization process. Dibenzothiophene can be removed completely under optimal reaction conditions, and no significant decrease in the catalytic activity of the catalyst was observed after 15 recycles [63].

Summary and outlook

In this paper, the synthesis and modifications of MCN in recent years have been made a brief review, which is expected to provide some guidance for future research on MCN. With the many advantages such as large surface area, narrow pore-size

distribution, convenient preparation, easy modification, non-toxicity, and environmental-friendliness, MCN has attracted increasing interest of researchers. It is believed that with in-depth research, MCN will be used in more ways, providing increasing convenience to our lives, and providing more help in resolving the problems of the environment and energy.

Acknowledgments This work was supported by grants from the National Nature Science Foundation of China (21407049), the Fundamental Research Funds for the Central Universities (222201314045), China Postdoctoral Science Foundation (2015T80409), and the Shanghai Pujiang Program (14PJ1402100).

Compliance with ethical standards

Conflict of interest The author(s) declare that they have no competing interests.

References

1. Z. Zhao, Y. Sun, F. Dong, Nanoscale **7**(1) (2015)
2. Y. Gu, Y. Zhang, X. Chang, Z. Tian, N. Chen, D. Shi, X. Zhang, L. Yuan, Sci. China Ser. A Math. **43**(2) (2000)
3. M. Laribi, R. Chenouf, K. Bachari, J. Hamani, Res. Chem. Intermed. **39**(4) (2013)
4. W. Yu, D. Xu, T. Peng, J. Mater. Chem. A. **19936**(3) (2015). doi:10.1039/C5TA05503B
5. J. Lei, Y. Chen, L. Wang, Y. Liu, J. Zhang, J. Mater. Sci. **50**(9) (2015)
6. J. Lei, Y. Chen, F. Shen, L. Wang, Y. Li, J. Zhang, J. Alloy. Compd. **631** (2015)
7. X. Jin, V.V. Balasubramanian, S.T. Selvan, D.P. Sawant, M.A. Chari, G.Q. Lu, A. Vinu, Angew. Chem. **121**(42) (2009)
8. H. Li, L. Zhou, L. Wang, Y. Liu, J. Lei, J. Zhang, Phys. Chem. Chem. Phys. **17**, 17406 (2015)
9. Y. Cui, J. Zhang, G. Zhang, J. Huang, P. Liu, M. Antonietti, X. Wang, J. Mater. Chem. **21**(34) (2011)
10. M.R. Wixom, J. Am. Ceram. Soc. **73**(7) (1990)
11. J. Liu, T. Sekine, T. Kobayashi, Solid State Commun. **137**(1) (2006)
12. H. Ma, X. Jia, L. Chen, P. Zhu, W. Guo, X. Guo, Y. Wang, S. Li, G. Zou, G. Zhang, J. Phys. Condens. Matter. **14**(44) (2002)
13. L. Galan, I. Montero, F. Rueda, Surf. Coat. Technol. **83**(1) (1996)
14. A. Hoffman, I. Gouzman, R. Brener, Appl. Phys. Lett. **64**(7) (1994)
15. H. Hofsäss, C. Ronning, U. Griesmeier, M. Gross, S. Reinke, M. Kuhr, Appl. Phys. Lett. **67**(1) (1995)
16. H. Song, F. Cui, X. He, W. Li, H. Li, J. Phys. Condens. Matter. **6**(31) (1994)
17. Z. Zhou, I. Bello, M. Lei, K. Li, C. Lee, S. Lee, Surf. Coat. Technol. **128**, 334 (2000)
18. T.Y. Yen, C.P. Chou, Appl. Phys. Lett. **67**(19) (1995)
19. A. Bousetta, M. Lu, A. Bensaoula, A. Schultz, Appl. Phys. Lett. **65**(6) (1994)
20. G. Yang, J. Wang, Appl. Phys. A **71**(3) (2000)
21. I. Mihailescu, E. Gyorgy, R. Alexandrescu, A. Luches, A. Perrone, C. Ghica, J. Werckmann, I. Cojocaru, V. Chumash, Thin Solid Films **323**(1) (1998)
22. A. Jabbari, H. Mahdavi, M. Nikoorazm, A. Ghorbani-Choghamarani, Res. Chem. Intermed. **41**, 5649 (2015)
23. J. Lei, L. Yang, D. Lu, X. Yan, C. Cheng, Y. Liu, L. Wang, J. Zhang, Adv. Opt. Mater. **3**(1) (2015)
24. J. Hu, Y. Zou, J. Liu, J. Sun, X. Yang, Q. Kan, J. Guan, Res. Chem. Intermed. **41**, 5703 (2015)
25. J. Lei, L. Wang, J. Zhang, ACS Nano **5**(5) (2011)
26. J. Lei, L. Wang, J. Zhang, Chem. Commun. **46**(44) (2010)
27. S. Xiao, G. Xu, G. Chen, X. Mu, Z. Chen, J. Zhu, Y. He, Res. Chem. Intermed. (2015). doi:10.1007/s11164-015-2017-2
28. T.-P. Fellinger, F. Hasché, P. Strasser, M. Antonietti. J. Am. Chem. Soc. **134**(9) (2012)
29. W. Shen, L. Ren, H. Zhou, S. Zhang, W. Fan, J. Mater. Chem. **21**(11) (2011)
30. A. Thomas, A. Fischer, F. Goettmann, M. Antonietti, J.-O. Müller, R. Schlögl, J.M. Carlsson, J. Mater. Chem. **18**(41) (2008)
31. P. Kuhn, M. Antonietti, A. Thomas, Angew. Chem. Int. Ed. **47**(18) (2008)

32. M. Hartmann, A. Vinu, Langmuir **18**(21) (2002)
33. A. Vinu, K. Ariga, T. Mori, T. Nakanishi, S. Hishita, D. Golberg, Y. Bando, Adv. Mater. **17**(13) (2005)
34. Z. Zhao, Y. Dai, J. Lin, G. Wang, Chem. Mater. **26**(10) (2014)
35. A. Vinu, Adv. Funct. Mater. **18**(5) (2008)
36. K.S. Lakhi, W.S. Cha, S. Joseph, B.J. Wood, S.S. Aldeyab, G. Lawrence, J.-H. Choy, A. Vinu, Catal. Today **243** (2015)
37. M.B. Ansari, H. Jin, M.N. Parvin, S.-E. Park, Catal. Today **185**(1) (2012)
38. G.P. Mane, D.S. Dhawale, C. Anand, K. Ariga, Q. Ji, M.A. Wahab, T. Mori, A. Vinu, J. Mater. Chem. A **1**(8) (2013)
39. S.N. Talapaneni, S. Anandan, G.P. Mane, C. Anand, D.S. Dhawale, S. Varghese, A. Mano, T. Mori, A. Vinu, J. Mater. Chem. **22**(19) (2012)
40. H. Yan, Chem. Commun. **48**(28) (2012)
41. Y. Wang, J. Zhang, X. Wang, M. Antonietti, H. Li, Angew. Chem. Int. Ed. **49**(19) (2010)
42. S. Min, G. Lu, J. Phys. Chem. C **116**(37) (2012)
43. S. Kumar, T. Surendar, B. Kumar, A. Baruah, V. Shanker, RSC Adv. **4**(16) (2014)
44. L. Shi, L. Liang, F. Wang, M. Liu, S. Zhong, J. Sun, Catal. Commun. **59** (2015)
45. K. Kailasam, J.D. Epping, A. Thomas, S. Losse, H. Junge, Energy Environ. Sci. **4**(11) (2011)
46. S. Yang, W. Zhou, C. Ge, X. Liu, Y. Fang, Z. Li, RSC Adv. **3**(16) (2013)
47. Y. Cui, J. Huang, X. Fu, X. Wang, Catal. Sci. Technol. **2**(7) (2012)
48. Y. Shiraishi, Y. Kofuji, H. Sakamoto, S. Tanaka, S. Ichikawa, T. Hirai, ACS Catal. **5**(5) (2015)
49. Q. Yang, W. Wang, Y. Zhao, J. Zhu, Y. Zhu, L. Wang, RSC Adv. **5**(68) (2015)
50. Y. Wang, X. Wang, M. Antonietti, Angew. Chem. Int. Ed. **51**(1) (2012)
51. M. Shalom, S. Inal, C. Fettkenhauer, D. Neher, M. Antonietti, J. Am. Chem. Soc. **135**(19) (2013)
52. J. Wei, J. Appl. Phys. **92**(11) (2002)
53. K. Datta, B. Reddy, K. Ariga, A. Vinu, Angew. Chem. Int. Ed. **49**(34) (2010)
54. Y. Wang, J. Yao, H. Li, D. Su, M. Antonietti, J. Am. Chem. Soc. **133**(8) (2011)
55. F.-F. Wang, S. Shao, C.-L. Liu, C.-L. Xu, R.-Z. Yang, W.-S. Dong, Chem. Eng. J. **264** (2015)
56. Y. Lu, Z. Wen, J. Jin, Y. Cui, M. Wu, S. Sun, J. Solid State Electr. **16**(5) (2012)
57. K. Kailasam, A. Fischer, G. Zhang, J. Zhang, M. Schwarze, M. Schröder, X. Wang, R. Schomäcker, A. Thomas, ChemSusChem. **8**(8) (2015)
58. J. Xu, Q. Jiang, T. Chen, F. Wu, Y.-X. Li, Catal. Sci. Technol. **5**(3) (2015)
59. A. Najafian, R. Rahimi, S. Zargari, M. Mahjoub-Moghaddas, A. Nazemi, Res. Chem. Intermed. (2015). doi:10.1007/S11164-015-2222-z
60. K. Takanabe, K. Kamata, X. Wang, M. Antonietti, J. Kubota, K. Domen, Phys. Chem. Chem. Phys. **12**(40) (2010)
61. B. Maleki, H. Eshghi, M. Barghamadi, N. Nasiri, A. Khojastehnezhad, S.S. Ashrafi, O. Pourshiani, Res. Chem. Intermed. (2015). doi:10.1007/S11164-015-2198-8
62. J. Chen, J. Li, Y. Zhang, S. Gao, Res. Chem. Intermed. **36**(8) (2010)
63. Y. Zhu, M. Zhu, L. Kang, F. Yu, B. Dai, Ind. Engin. Chem. Res. **54**(7) (2015)